



LETTER • OPEN ACCESS

## Spatial optimality and temporal variability in Australia's wind resource

To cite this article: Andrew Gunn *et al* 2023 *Environ. Res. Lett.* **18** 114048

View the [article online](#) for updates and enhancements.

You may also like

- [TERN. Australia's land observatory: addressing the global challenge of forecasting ecosystem responses to climate variability and change](#)  
James Cleverly, Derek Eamus, Will Edwards et al.
- [Creating past habitat maps to quantify local extirpation of Australian threatened birds](#)  
Michelle Ward, James E M Watson, Hugh P Possingham et al.
- [Characterisation and mitigation of renewable droughts in the Australian National Electricity Market](#)  
Andy Boston, Geoffrey D Bongers and Nathan Bongers

ENVIRONMENTAL RESEARCH  
LETTERS

## LETTER

## OPEN ACCESS

RECEIVED  
7 April 2023REVISED  
24 September 2023ACCEPTED FOR PUBLICATION  
11 October 2023PUBLISHED  
27 October 2023

Original Content from  
this work may be used  
under the terms of the  
[Creative Commons  
Attribution 4.0 licence](#).

Any further distribution  
of this work must  
maintain attribution to  
the author(s) and the title  
of the work, journal  
citation and DOI.



## Spatial optimality and temporal variability in Australia's wind resource

Andrew Gunn<sup>1,\*</sup>, Roger Dargaville<sup>2</sup>, Christian Jakob<sup>1,3</sup> and Shayne McGregor<sup>1,3</sup><sup>1</sup> School of Earth, Atmosphere & Environment, Monash University, Clayton, Australia<sup>2</sup> Department of Civil Engineering, Monash University, Clayton, Australia<sup>3</sup> ARC Centre of Excellence for Climate Extremes, Monash University, Clayton, Australia

\* Author to whom any correspondence should be addressed.

E-mail: [a.gunn@monash.edu](mailto:a.gunn@monash.edu)**Keywords:** wind power, climate variability, optimisationSupplementary material for this article is available [online](#)

## Abstract

To meet electricity demand using renewable energy supply, wind farm locations should be chosen to minimise variability in output, especially at night when solar photovoltaics cannot be relied upon. Wind farm location must balance grid-proximity, resource potential, and wind correlation between farms. A top-down planning approach for farm locations can mitigate demand unmet by wind supply, yet the present Australian wind energy market has bottom-up short-term planning. Here we show a computationally tractable method for optimising farm locations to maximise total supply. We find that Australia's currently operational and planned wind farms produce less power with more variability than a hypothetical optimal set of farms with equivalent capacity within 100 km of the Australian Energy Market Operator grid. Regardless of the superior output, this hypothetical set is still subject to variability due to large-scale weather correlated with climate modes (i.e. El Niño). We study multiple scenarios and highlight several internationally transferable planning implications.

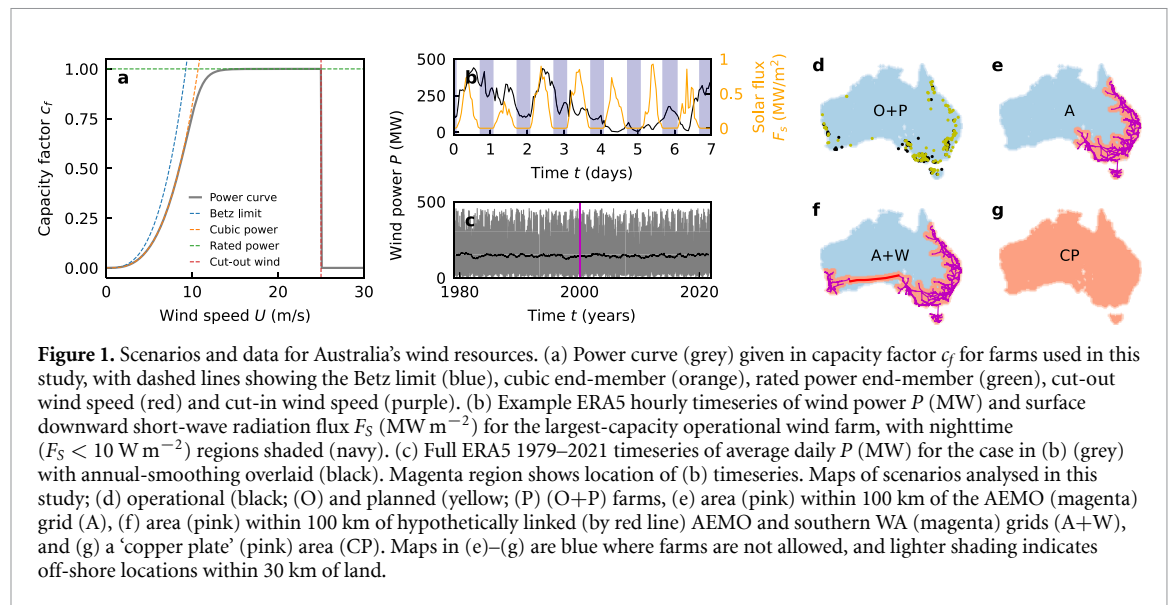
## 1. Introduction

Energy supply is changing from non-renewable to renewable sources globally [1]. In 2021, 29% of Australia's energy supply came from renewable sources, up from 8% in 2001 [2]. In a scenario where supply is entirely renewable, meeting demand with these sources requires new planning approaches [3–6]. The current power grid manifests from population density and sites of large stores of on-demand non-renewable supply [2, 7], and owing to Australia's climate and geography, non-dispatchable renewable sources (solar photovoltaics and wind) are more feasible over most of the nation than dispatchable stored renewable sources [2, 8–11] (e.g. bioenergy and hydro-schemes). To minimise energy storage costs while meeting demand, a blend of daytime solar and night-time wind power will be necessary [12, 13]. Ideally minimum wind supply at night should meet baseload demand [1, 3–5].

Finding a set of wind farms that meets this demand is an optimisation problem [7, 14–20].

Each individual wind farm experiences a timeseries of local weather and climate which alone cannot always meet demand. Choosing locations with minimal correlation in wind power potential between them will create more consistent aggregated output [21–27], however these locations may not necessarily have strong winds, and for many farms this choice becomes quickly intractable. For example, there are around as many combinations of placing 97 farms (number currently operating connected to the Australian Energy Market Operator (AEMO) grid) in 300 prospective locations as there are atoms in the Universe ( $^{300}C_{97} \approx 10^{80}$ ). This problem must also consider myriad other factors, including the proximity of prospective farm locations to the energy grid to minimise transmission costs and energy losses [7, 9, 16, 17, 19, 20].

The existing set of 97 operational wind farms in Australia connected to the power grid—which have a total capacity of 10.3 GW—were not chosen with a top-down optimality approach, rather each location was chosen with the goal of maximising return



on investment for that particular farm. In addition to the existing farms, as of 2022 there are 150 farms currently in some planning stage totalling 113.2 GW capacity. The capacity of these farms (figure S1), like the population and power grid, is overwhelmingly concentrated in the southeast of the country (figure 1(d)). The locations of these farms are chosen within a legal framework and are approved by energy market operators, but largely are selected based on sub-decadal assessments of local wind resource potential, land ownership and the interests of the farm's stakeholders [14–17, 19]. This process does not necessarily create optimal wind power supply for the grid and, given the  $\sim 20$ –30 year life cycle of farms [28], can create lasting inefficiencies.

Regardless of the spatial configuration of a set of wind farms within a region, there is unmitigable variation in the wind itself [22, 29–31]. At the sub-farm scale variability can occur due to local topography [32–34], or extreme winds posing a hazard to infrastructure [1, 13, 33, 35], while at the intra-farm scale large weather or climate modes can create significant changes in wind supply which persist for days to many years [29, 36–41]. For all locations, wind speeds in the atmospheric boundary layer have approximately Weibull distributions (a peak with a long right tail) and often a diurnal cycle [3, 31]. This last point is particularly relevant for night-time wind supply, since there is an increased advantage in higher turbine hub heights to access the nocturnal jet over the slow, stably stratified near-surface flow [42–45]. In general, the wind speed at hub height can be mapped onto a capacity factor  $c_f$  (i.e. the proportion of the turbine rated capacity power produced) using a 'power curve' [1, 7, 20]. Typical power curves rise after a 'cut-in' wind speed with a wind speed cubed relationship before plateauing at the turbine's

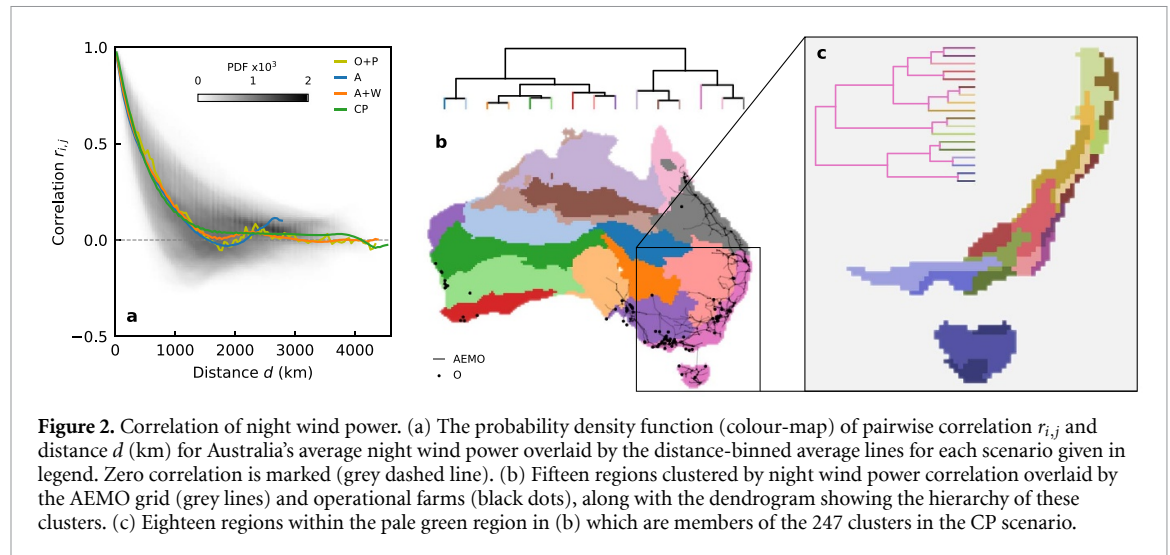
maximum capacity, and are zero after a 'cut-out' speed (figures 1(a) and S2; Methods).

In this study we compare supply from Australia's operational and planned wind farms to a hypothetical set of wind farms chosen to optimise night-time supply. We employ 43 years (1979–2021) of wind data at 100 m height above ground level from the ECMWF Reanalysis 5th Generation (ERA5) reanalysis at  $0.25^\circ$  spatial and 1-hour temporal resolution [46] to conduct the comparison and assess the viability of Australia's wind resource (figure 1(b); Methods). In each distinct area of interest (within 100 km of the AEMO grid, figure 1(e); a hypothetically linked AEMO and southern Western Australia grid, figure 1f; or a 'copper plate' grid anywhere in Australia, figure 1(g)), we use a correlation clustering algorithm to select a hypothetical set of farms with a total capacity equal to that of the operational and planned wind farms. Each of the farms in these hypothetical sets have an individual capacity of 500 MW, such that the total number of farms matches the operational and planned set ( $N = 247$ ; 123.5 GW total capacity). Our analysis has two central results: (1) existing methods of optimal set selection can miss more cost-effective and powerful sets, and (2) there exists a significant unmitigable variability in supply which is attributable to larger-scale climate variability.

## 2. Results

### 2.1. Set selection

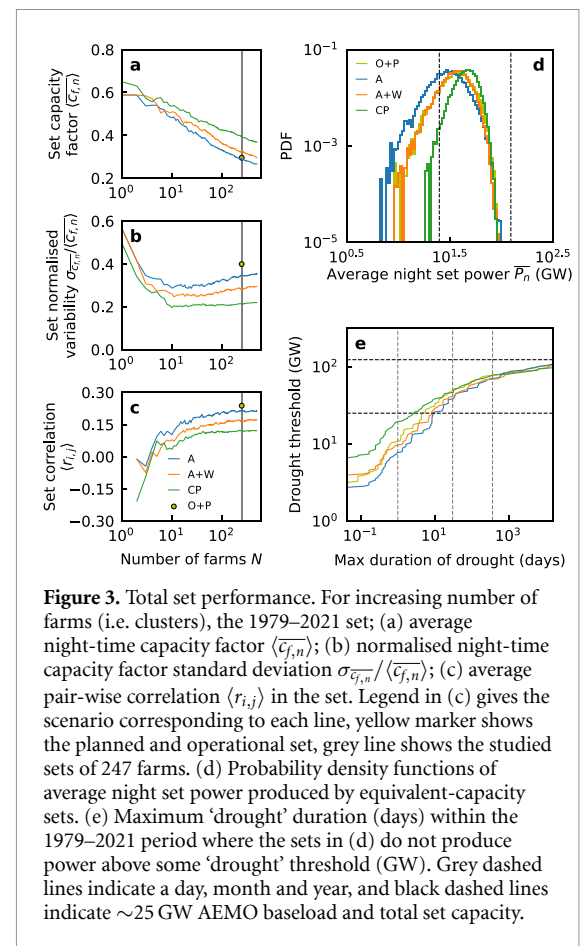
We consider each point in the ERA5 reanalysis grid as a potential distinct location for a wind farm and produce a cross-correlation matrix of the daily night-time average capacity factor timeseries over the 1979–2021 period for the points. We then organise these points into clusters, where clusters are



chosen such that points are more similar to other points within them than to points in other clusters (using a farthest point algorithm; Methods). The measure of dissimilarity between sites is the  $L^2$ -norm (i.e. Euclidean distance) in the correlation space with dimensions equal to the number of points. This clustering method is hierarchical and nested: to split a domain into  $N + 1$  clusters, the cluster with points least correlated within itself in a set of  $N$  clusters is split in two (as reflected in a dendrogram). In this study, we choose a hypothetical set as each site with the maximum average night-time capacity factor within 247 clusters, equal to the number of hypothetical farms.

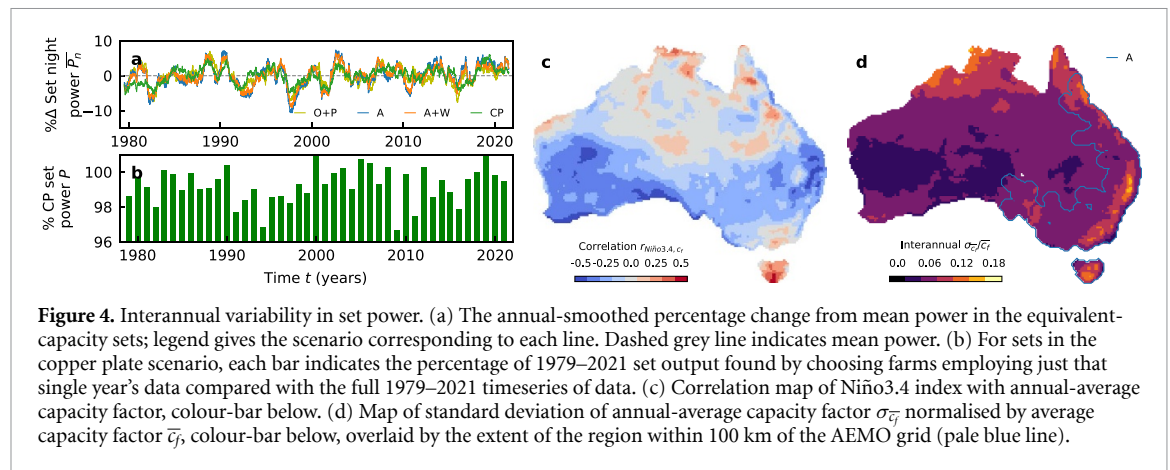
This clustering method, novel to wind farm optimisation but common in other sciences such as genetics and image analysis, reveals the primary issue facing Australia's operational wind supply: most of the currently operational capacity lies within a correlated region extending across Tasmania and the southeast coast of mainland Australia [7]. To illustrate this, in figure 2(b) we plot the 'copper plate' (CP) scenario split into 15 correlated clusters—night-time wind power in the pink region is more correlated with itself than anywhere else. In figure 2(c), we show the nested regions within the pink region, each of which contains one of the 247 farms in the CP hypothetical set. Furthermore, the AEMO grid covers just 7 of the 15 regions in figure 2(b).

The method also reveals the information lost by the most common alternative technique for optimal set selection; the mean pair-wise correlation-distance function [7, 34, 39, 47] (figure 2(a)). Often a length-scale characterising the decay in the average pair-wise correlation-distance function is defined as the minimum distance between farms [7, 34, 39, 47], yet this disguises key results of the clustering analysis; correlated regions do not have to be the same shape or size, or even contiguous (figure 2(b)). In figure 2(a) we plot the average correlation-distance functions



for each scenario over the total CP probability density function, showing that not allowing farms within some decay length-scale would omit many potential pairs which are anti-correlated.

Hypothetical sets of equivalent total capacity have the same or higher average supply (intercept with grey line in figure 3(a)) than the currently operational and planned set (O+P; yellow dot in figure 3(a)). For sets selected with the clustering strategy, this leads to an



optimum set size—around ten farms—for variability relative to power (figure 3(b)), where the gain from minimising the set correlation is weakened least by including farms more variable relative to their power (figures 3(a) and (c)). We find that all hypothetical sets outperform their operational plus planned set counterpart with equal capacity (figures 3(a)–(c)). In figure S3 and table S1 we extend this analysis to compare hypothetical sets of varying farm capacities to just the existing operational farms, finding similar results.

In figures 3(d) and (e) we show the performance of the sets statistically. The probability distributions of daily night-time average set power are narrower and peak higher for the most spatially disperse sets (figure 3(d)). These highly asymmetric PDFs show the modal night-time supply is below the average night-time supply. Another way of assessing the skewed power output of these sets is by calculating the duration of ‘wind droughts’ (i.e. periods where the set does not supply power above some threshold) in the 1979–2021 observation period [21, 38]. Figure 3(e) shows the maximum duration of contiguous time (in hour increments, due to the time-step of the ERA5 reanalysis) the total wind supply from a set never exceed some threshold amount over the 42 year observation period. The similarity of these curves for different sets for long drought lengths hints at the role of unmitigable climate variability in times of poor wind resource potential. For example, in all cases, total wind supply from the set never exceeds 44% of its capacity in any hour for an entire month in 1979–2021 (March of 1982).

## 2.2. Climate variability

To investigate this temporal variability, we look at annual-smoothed timeseries of change around the mean set output (figure 4(a)). Despite hypothetical sets being chosen to minimise variability in total output by selecting uncorrelated farms, there are still  $>10\%$  changes in supply between consecutive years. These are generally smaller than the operational and planned set for equivalent capacity, but

at times are clearly driven by the same variability in the climate. The El Niño Southern Oscillation climate mode has large influence over interannual variability in many aspects of Australian climate and, indeed, energy demand and supply [2, 18, 36, 37, 41]. We plot a correlation map between the annual averages of capacity factor and the Niño3.4 index which quantifies El Niño Southern Oscillation, finding La Niña generally produces stronger wind supply in Australia [39], while the spatial signature shows the strongest absolute correlations exist nearer the coast (figure 4(c)).

The above analysis shows large year-to-year variability in power output due to intrinsic variability in the winds. This means that planning wind farm locations using short records of a few years can be very misleading as to what capacity is needed. In addition, the identification of minimally correlated regions likely also depends on the amount of data used; in this study we have used 43 years of data—near the typical life of a wind farm. We investigate this by repeating the clustering described above for individual years. We show the total set power for the copper plate hypothetical set if just a single year of data was used to find the set configuration, as a percentage of the power from when all 43 years of data is used (figure 4(b)). Around 1% of power is lost, up to 4% varying across years.

At the farm-level, we plot a map of the standard deviation in annual average capacity factor normalised by the average capacity factor, with the extent of area within 100 km of the AEMO grid overlaid (figure 4(d)). We find that the highest interannual variability at a site in Australia is 16% of its mean; half the variation in average capacity factors across Australia spatially (32% of the average).

## 3. Discussion

There are a few important caveats to this study. Foremost, the ERA5 reanalysis is not a perfect representation of past weather [30, 44–46, 48, 49], and the spatial resolution does not allow access to fine-scale



topographic effects which are important for farm site selection [32–34]. We also chose equal-capacity farms in the hypothetical sets—a constraint which could be relaxed and optimised—and did not account for losses due to scale-dependent collective turbine wakes [1, 50–52]. While we considered proximity to the power grid, we did not incorporate any costs or penalties for supply as a function of grid proximity which would be relevant in a Levelised Cost of Energy analysis [7, 19], or land-use and government planning restrictions. These assumptions, however, do not preclude the main findings we present, which are principally a proof-of-concept of a generic approach to optimal site selection and assessing the role of large-scale variability in climate on wind supply. These findings are readily applicable to other energy markets, and climate datasets such as regional (e.g. BARRA [48]) or higher-resolution (e.g. ERA5-Land [49]) reanalyses.

This study raises some important points for national energy market planning. Increasing the spatial coverage of power grids is essential for a cost-effective transition to renewables [2, 3, 10, 18, 21, 23]. We find that hypothetical sets in the scenario where farms are within 100 km of a connected AEMO and southern WA power grid produce on average 12% more power than within 100 km of the AEMO grid alone with equivalent total capacity (figure 3(a)). We also find that despite the progress in wind supply, now accounting for 13% of total energy supply on the AEMO grid in 2021, optimally-selected farms within 100 km of the AEMO grid could produce the same as the operational and planned farm supply with a 13% increase in consistency using equivalent capacity (figures 3(a) and (b)), and farms of reasonable size within 100 km of the AEMO grid could produce 35% more supply than the existing operational farms with a 39% increase in consistency using equivalent capacity (figure S3a, table S1). This is somewhat attributable to top-down strategy, however we also showed how sites assessed with one year of wind observations may underperform over a farm life cycle by up to 16% due to interannual variability in local wind climate (figure 4(d)). Wind farm stakeholders take on significant risk with short site assessments.

We also found that achieving average night-time power consistently above baseload ( $\sim 25$  GW for AEMO) with wind supply is not feasible, even with strategically selected farms, owing to large-scale coherent features in wind climate (figure 3(c)). Including all planned additional capacity, however, does reduce these droughts to only a few days (figure 3(e)), a dramatic improvement over the presently operational set where supply did not exceed 6 GW at any hour lasted for over 3 months (figure 4(c)). This lack of on-demand power, especially at night, highlights the need for stored energy given our present demand [3, 4, 8]. Finally, we find that there is little performance lost in hypothetical

sets when selecting sites iteratively rather than as a collective, since the primary control on performance is power grid extent (figures 3(a)–(c)). Interannual variability in wind resource is significant and spatially correlated (figure 4(d)) and therefore, even for a perfectly designed set of wind farm locations, exerts a strong control on wind supply (figure 4(a)) [41].

Future work can take this study in several directions. Australia-specific policy choices or site assessment could be informed by a tailored version of this analysis with narrower scope. Detailed assessments of the advantages of the nocturnal and off-shore boundary layers for wind resources [36, 42, 44], which extend beyond the single-turbine scale and contextualise wind supply with demand and solar, may help inform future resource allocation. Our preliminary findings on diurnal variability suggest offshore sites tend to provide higher power but do not have relatively strong night-time power (to be expected with the higher ocean heat capacity), and that power is slightly more variable at night offshore (figure S4). More broadly, a framework, perhaps borrowed from other climate studies, for attribution of wind droughts to predictable climate states could help provide lead-time for ramping up alternative supply sources [30, 36–40]. We also believe that the clustering analysis outlined here could be a useful tool in studies of other aspects of climate. Finally, the climate system is changing on a timescale well within the life cycle of wind farms with unclear effects on wind; to what extent this influences the renewable energy transition must be assessed [8, 53].

## 4. Methods

### 4.1. Power curve

We convert wind speed  $U$  ( $\text{m s}^{-1}$ ) data into capacity factor  $c_f$  using the grey curve in figure 1(a). Above the cut-out speed  $U_1 = 25$  ( $\text{m s}^{-1}$ ) there is no power generated (for turbine safety):  $c_f(U \geq U_1) = 0$ . For below cut-out speed winds,  $U < U_1$ , the power ramps up like the cube of the wind speed,  $c_f = f(U) = A(U)^3$ , then saturates at  $c_f = g(U) = 1$ . The factor  $A$  is found using typical parameters for turbines:  $A = C_B \rho_f \pi L^2 e / 2C$ , where;  $C_B = 16/27$  is the Betz constant setting the theoretical maximum power extraction,  $\rho_f = 1.2$  ( $\text{kg m}^{-3}$ ) is the air density,  $L = 150/2$  (m) is the blade length,  $e = 0.65$  is a typical turbine efficiency, and  $C = 5$  MW is a typical modern turbine rated capacity [7]. We blend the cubic  $f$  and saturated  $g$  behaviour with a spline function,  $c_f(U - U_0) = (f(U - U_0))^{-\beta} + g(U - U_0)^{-\beta})^{-1/\beta}$ , where  $\beta = 5$  sets the sharpness of the transition between the functions  $f$  and  $g$ . All capacity factors computed from reanalysis wind data are then scaled by farm capacities when required to produce power values. A comparison of this curve to real turbine capacity factor curves is given in figure S2.

#### 4.2. ERA5 reanalysis

We used 0.25° resolution ERA5 reanalysis data [46] for hourly instantaneous wind speeds at 100 meters for the period 1979–2021 (inclusive) to attain capacity factors using the power curve explained in the previous Methods section. We further used the hourly average surface downward short-wave radiation flux to mask out periods where co-located solar supply would not produce power, and classified those as nighttime with a threshold flux of 10 W m<sup>-2</sup>. For each day (UTC), the daily average capacity factors and nighttime-only average capacity factors were analysed. Spatially, ERA5 data was masked according to the model's native land-sea mask, cropped specifically to Australia. Offshore regions were included in the analysis by extending this land-sea mask 2 grid-points (i.e. approximately 30 km) beyond the land edge. The mask is then adjusted to the scenario based on a 100 km range to the closest line on the power grid. This method is implemented with Xarray [54], NumPy [55] and Shapely [56].

#### 4.3. Operational and planned farms

Operational and planned farm data was collected as explained in the data availability statement and is given in table S2. These farms have known total capacities but each farms turbine-weighted power curve and hub-height is not known. We assumed that their performance was equivalent to the hypothetical farms, such that we used the same 100 m winds and power curve to attain a capacity factor, then multiplied this by the total farm capacity. These capacity factors were attained using the data from the ERA5 grid point closest to the farm location. Some farms lie closest to the same ERA5 grid point but are treated independently.

#### 4.4. Correlation clustering

Correlation values were found between each pair of timeseries for daily-average nighttime capacity factors for 1979–2021. This correlation matrix, with size ( $X, X$ ) where  $X$  is the number of grid points, gives each location a coordinate in a space spanned by  $X$  dimensions. The distance between points  $m$  and  $n$  in this space is defined as  $d_{m,n} = \sqrt{\sum_i^X (m_i - n_i)^2}$ , i.e. the Euclidean distance or L<sup>2</sup>-norm. Locations can then be clustered by looking at their distances from each other in this space. We use a farthest point algorithm (referred to as 'complete' in figure S5) to cluster points, which merges clusters that have the smallest distance  $D$  between the farthest point in one cluster  $A$  from a point in another cluster  $B$ :  $D = \max\{d_{m,n}\}$ , where  $A$  contains points  $m$  and  $B$  contains points  $n$ . In this study clusters are formed by iterative merging in a hierarchical fashion up to a prescribed number of clusters. The spatial sites are then labelled by the cluster they belong to and a cluster map can be produced. A comparison of the clustering

algorithm we use to alternatives is given in figure S5, and example truncated dendrograms for clusters formed in each scenario is given in figure S6. This method is implemented with SciPy [57].

#### Data availability statement

The ERA5 reanalysis data used in this study are available in the Climate Data Store database <https://cds.climate.copernicus.eu/>. The Niño3.4 index data used in this study are available on the NOAA ERS Physical Sciences Laboratory site [https://psl.noaa.gov/gcos\\_wgsp/Timeseries/Nino34/](https://psl.noaa.gov/gcos_wgsp/Timeseries/Nino34/). The operational wind farm data used in this study are available on the AEMO National Electricity Market Dashboard <https://aemo.com.au/Energy-systems/Electricity/National-Electricity-Market-NEM/Data-NEM/Data-Dashboard-NEM>. The planned wind farm data used in this study are available on the EcoGeneration site [www.ecogeneration.com.au/wp-content/uploads/2022/02/ECO-WindMap-2022.pdf](http://www.ecogeneration.com.au/wp-content/uploads/2022/02/ECO-WindMap-2022.pdf). All operational and planned wind farm data used in this study is collated in table S2. The power grid data used in this study are available from the Australian Government data site <https://data.gov.au/dataset/ds-ga-1185c97c-c042-be90-e053-12a3070a969b/details?q=transmission%20lines>. The turbine data used to estimate the power curve are available from the Open Energy Platform site [https://openenergy-platform.org/dataedit/view/supply/wind\\_turbine\\_library](https://openenergy-platform.org/dataedit/view/supply/wind_turbine_library). The adapted power grid for scenario 'A+W' data are available at <https://github.com/geomorphlab/wind-power>.

#### Acknowledgments

This research was undertaken with the assistance of resources from the National Computational Infrastructure (NCI Australia), an NCRIS enabled capability supported by the Australian Government. We thank Julie Hughes at Paragon Media for collated data on planned wind farms in Australia. C J and S M acknowledge funding from the Australian Research Council through the Centre of Excellence for Climate Extremes (#CE170100023).

#### Code availability

Code to reproduce this paper can be found at <https://doi.org/10.5281/zenodo.8368760>.

#### Author contributions

Formal Analysis, Software, Validation, Visualization, Data Curation, Project Administration, Investigation and Writing—original draft, A G; Resources, Supervision, Conceptualization, Methodology, Funding Acquisition and Writing—review and editing; all authors.

## Conflict of interests

The authors declare no competing interests.

## References

- [1] Veers P *et al* 2019 Grand challenges in the science of wind energy *Science* **366** eaau2027
- [2] Operator A E M 2022 2022 integrated system plan for the national electricity market AEMO
- [3] Shaner M R, Davis S J, Lewis N S and Caldeira K 2018 Geophysical constraints on the reliability of solar and wind power in the United States *Energy Environ. Sci.* **11** 914–25
- [4] Rugolo J and Aziz M J 2012 Electricity storage for intermittent renewable sources *Energy Environ. Sci.* **5** 7151–60
- [5] Heptonstall P J and Gross R J 2021 A systematic review of the costs and impacts of integrating variable renewables into power grids *Nat. Energy* **6** 72–83
- [6] MacGill I 2010 Electricity market design for facilitating the integration of wind energy: experience and prospects with the Australian National Electricity Market *Energy Policy* **38** 3180–91
- [7] Huva R, Dargaville R and Rayner P 2016 Optimising the deployment of renewable resources for the Australian NEM (National Electricity Market) and the effect of atmospheric length scales *Energy* **96** 468–73
- [8] Evans J P, Kay M, Prasad A and Pitman A 2018 The resilience of Australian wind energy to climate change *Environ. Res. Lett.* **13** 024014
- [9] Diesendorf M 2006 Wind power in Australia *Int. J. Environ. Stud.* **63** 765–76
- [10] Valentine S 2010 Braking wind in Australia: a critical evaluation of the renewable energy target *Energy Policy* **38** 3668–75
- [11] Prasad A A, Taylor R A and Kay M 2017 Assessment of solar and wind resource synergy in Australia *Appl. Energy* **190** 354–67
- [12] Cutler N J, Boerema N D, MacGill I F and Outhred H R 2011 High penetration wind generation impacts on spot prices in the Australian national electricity market *Energy Policy* **39** 5939–49
- [13] Cutler N, Kay M, Outhred H and MacGill I 2007 High-risk scenarios for wind power forecasting in Australia *Proc. European Wind Energy Conf.*
- [14] Weinand J M, Naber E, McKenna R, Lehmann P, Kotzur L and Stolten D 2022 Historic drivers of onshore wind power and inevitable future trade-offs *Environ. Res. Lett.* **17** 074018
- [15] Drechsler M, Egerer J, Lange M, Masurowski F, Meyerhoff J and Oehlmann M 2017 Efficient and equitable spatial allocation of renewable power plants at the country scale *Nat. Energy* **2** 1–9
- [16] Huenteler J, Tang T, Chan G and Anadon L D 2018 Why is China's wind power generation not living up to its potential? *Environ. Res. Lett.* **13** 044001
- [17] Lu X, McElroy M B, Peng W, Liu S, Nielsen C P and Wang H 2016 Challenges faced by China compared with the US in developing wind power *Nat. Energy* **1** 1–6
- [18] Kiss P and János I 2008 Limitations of wind power availability over Europe: a conceptual study *Nonlinear Process. Geophys.* **15** 803–13
- [19] Ali S, Lee S-M and Jang C-M 2017 Determination of the most optimal on-shore wind farm site location using a GIS-MCDM methodology: evaluating the case of South Korea *Energies* **10** 2072
- [20] Davidson M R, Zhang D, Xiong W, Zhang X and Karplus V J 2016 Modelling the potential for wind energy integration on China's coal-heavy electricity grid *Nat. Energy* **1** 1–7
- [21] Fertig E, Apt J, Jaramillo P and Katzenstein W 2012 The effect of long-distance interconnection on wind power variability *Environ. Res. Lett.* **7** 034017
- [22] Bandi M M 2017 Spectrum of wind power fluctuations *Phys. Rev. Lett.* **118** 028301
- [23] Mauch B, Apt J, Carvalho P M and Jaramillo P 2013 What day-ahead reserves are needed in electric grids with high levels of wind power? *Environ. Res. Lett.* **8** 034013
- [24] Caralis G, Perivolaris Y, Rados K and Zervos A 2008 On the effect of spatial dispersion of wind power plants on the wind energy capacity credit in Greece *Environ. Res. Lett.* **3** 015003
- [25] Holttinen H 2008 Estimating the impacts of wind power on power systems—summary of IEA Wind collaboration *Environ. Res. Lett.* **3** 025001
- [26] Hu S, Xiang Y, Zhang H, Xie S, Li J, Gu C, Sun W and Liu J 2021 Hybrid forecasting method for wind power integrating spatial correlation and corrected numerical weather prediction *Appl. Energy* **293** 116951
- [27] Hallgren W, Gunturu U B and Schlosser A 2014 The potential wind power resource in Australia: a new perspective *PLoS One* **9** e99608
- [28] Judge F, McAuliffe F D, Sperstad I B, Chester R, Flannery B, Lynch K and Murphy J 2019 A lifecycle financial analysis model for offshore wind farms *Renew. Sustain. Energy Rev.* **103** 370–83
- [29] Charakopoulos A, Karakasidis T and Sarris L 2019 Pattern identification for wind power forecasting via complex network and recurrence plot time series analysis *Energy Policy* **133** 110934
- [30] Olson J B *et al* 2019 Improving wind energy forecasting through numerical weather prediction model development *Bull. Am. Meteorol. Soc.* **100** 2201–20
- [31] Zhou Y and Smith S J 2013 Spatial and temporal patterns of global onshore wind speed distribution *Environ. Res. Lett.* **8** 034029
- [32] Pickering B, Grams C M and Pfenninger S 2020 Sub-national variability of wind power generation in complex terrain and its correlation with large-scale meteorology *Environ. Res. Lett.* **15** 044025
- [33] Lange J, Mann J, Berg J, Parvu D, Kilpatrick R, Costache A, Chowdhury J, Siddiqui K and Hangan H 2017 For wind turbines in complex terrain, the devil is in the detail *Environ. Res. Lett.* **12** 094020
- [34] Olauson J and Bergkvist M 2016 Correlation between wind power generation in the European countries *Energy* **114** 663–70
- [35] Pryor S C and Barthelmie R J 2021 A global assessment of extreme wind speeds for wind energy applications *Nat. Energy* **6** 268–76
- [36] van der Wiel K, Bloomfield H C, Lee R W, Stoop L P, Blackport R, Screen J A and Selten F M 2019 The influence of weather regimes on European renewable energy production and demand *Environ. Res. Lett.* **14** 094010
- [37] Thornton H E, Scaife A A, Hoskins B J and Brayshaw D J 2017 The relationship between wind power, electricity demand and winter weather patterns in Great Britain *Environ. Res. Lett.* **12** 064017
- [38] Ohlendorf N and Schill W-P 2020 Frequency and duration of low-wind-power events in Germany *Environ. Res. Lett.* **15** 084045
- [39] Martin C M S, Lundquist J K and Handschy M A 2015 Variability of interconnected wind plants: correlation length and its dependence on variability time scale *Environ. Res. Lett.* **10** 044004
- [40] Richardson D, Pitman A J and Ridder N N 2023 Climate controls on compound solar and wind droughts in Australia *EarthArXiv* (available at: <https://doi.org/10.31223/X5W09W>)
- [41] Gunturu U B and Hallgren W 2017 Asynchrony of wind and hydropower resources in Australia *Sci. Rep.* **7** 8818
- [42] Wharton S and Lundquist J K 2012 Atmospheric stability affects wind turbine power collection *Environ. Res. Lett.* **7** 014005
- [43] Vanderwende B J and Lundquist J K 2012 The modification of wind turbine performance by statistically distinct atmospheric regimes *Environ. Res. Lett.* **7** 034035



- [44] Soares P M, Lima D C and Nogueira M 2020 Global offshore wind energy resources using the new ERA-5 reanalysis *Environ. Res. Lett.* **15** 1040a2
- [45] Torralba V, Doblas-Reyes F J and Gonzalez-Reviriego N 2017 Uncertainty in recent near-surface wind speed trends: a global reanalysis intercomparison *Environ. Res. Lett.* **12** 114019
- [46] Hersbach H *et al* 2020 The ERA5 global reanalysis *Q. J. R. Meteorol. Soc.* **146** 1999–2049
- [47] Ren G, Wan J, Liu J and Yu D 2020 Spatial and temporal correlation analysis of wind power between different provinces in China *Energy* **191** 116514
- [48] Su C-H *et al* 2019 BARRA v1.0: the Bureau of Meteorology atmospheric high-resolution regional reanalysis for Australia *Geosci. Model Dev.* **12** 2049–68
- [49] Muñoz-Sabater J *et al* 2021 ERA5-Land: a state-of-the-art global reanalysis dataset for land applications *Earth Syst. Sci. Data* **13** 4349–83
- [50] Volker P J, Hahmann A N, Badger J and Jørgensen H E 2017 Prospects for generating electricity by large onshore and offshore wind farms *Environ. Res. Lett.* **12** 034022
- [51] Lundquist J, DuVivier K, Kaffine D and Tomaszewski J 2019 Costs and consequences of wind turbine wake effects arising from uncoordinated wind energy development *Nat. Energy* **4** 26–34
- [52] Possner A and Caldeira K 2017 Geophysical potential for wind energy over the open oceans *Proc. Natl Acad. Sci.* **114** 11338–43
- [53] Devis A, Van Lipzig N P and Demuzere M 2018 Should future wind speed changes be taken into account in wind farm development? *Environ. Res. Lett.* **13** 064012
- [54] Hoyer S and Hamman J 2017 xarray: N-D labeled arrays and datasets in python *J. Open Res. Softw.* **5** 10
- [55] Harris C R *et al* 2020 Array programming with NumPy *Nature* **585** 357–62
- [56] Gillies S 2013 The shapely user manual *PyPi* (available at: [https://sethcs23.github.io/wiki/Python/The\\_Shapely\\_User\\_Manual\\_%E2%80%94Shapely\\_1.2\\_and\\_1.3\\_documentation.pdf](https://sethcs23.github.io/wiki/Python/The_Shapely_User_Manual_%E2%80%94Shapely_1.2_and_1.3_documentation.pdf))
- [57] Virtanen P *et al* 2020 SciPy 1.0: fundamental algorithms for scientific computing in Python *Nat. Methods* **17** 261–72